M31 Planetary nebulae as seen by the Panchromatic Hubble Andromeda Treasury

Philip A. Rosenfield¹, L. Clifton Johnson¹, Léo Girardi², Julianne J. Dalcanton¹, Benjamin F. Williams¹, Luciana Bianchi³, Paola Marigo⁴, Nelson Caldwell⁵, Anil C. Seth⁶, Karl Gordon⁷, and Dustin Lang⁸ for the PHAT Team

¹Department of Astronomy, University of Washington, Box 351580, Seattle, WA 98195, USA

²Osservatorio Astronomico di Padova – INAF, Vicolo dell'Osservatorio 5, I-35122 Padova, Italy

³Department of Physics and Astronomy, Johns Hopkins University, Baltimore, MD 21218, USA

> ⁴Dipartimento di Astronomia, Universitá di Padova, Vicolo dell'Osservatorio 2, 35122 Padova, Italy

⁵Harvard-Smithsonian Center for Astrophysics, 60 Garden Street Cambridge, MA 02138, USA

⁶Department of Physics & Astronomy, University of Utah, Salt Lake City, UT 84112, USA
⁷Space Telescope Science Institute, MD 21218, USA

⁸Department of Astrophysical Sciences, Princeton University, Princeton, NJ 08544, USA

Abstract. We present a preliminary analysis of known planetary nebulae (PNe) in M31 that were observed in the first year of the Panchromatic Hubble Andromeda Treasury HST Multi-cycle program. We use the properties of this sample to discuss PNe from this new multi-band survey.

Keywords. stars: evolution, stars: AGB and post-AGB, planetary nebulae: general, galaxies: individual (M31)

1. Introduction

The Andromeda Galaxy is the nearest giant galaxy and is rich with planetary nebulae (PNe; e.g., Ciardullo *et al.* 1989; Merrett *et al.* 2006). The Panchromatic Hubble Andromeda Treasury (PHAT) is a Hubble Space Telescope (HST) Multi-cycle program that will image roughly one third of M31's star-forming disk in six filters from UV to IR. As a result, PHAT will enable M31 to be a fundamental calibrator of stellar evolution and star-formation processes.

Although not primarily designed to study PNe, PHAT provides accurate photometry in 6 filters, including HST/ACS F475W, which covers the [O III] 5007Å emission line. Thus, the PHAT survey offers the wavelength coverage, the large spatial resolution, and the high astrometric accuracy needed to study M31's PNe population across the radial extent of its bulge and disk.

We briefly describe the results from a preliminary analysis of PNe observed in the first year of the PHAT survey.

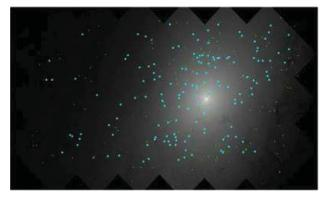


Figure 1. Spatial distribution of M06 Cataloged PNe (green) and sources matched to PHAT photometry (cyan) overlaid on a F475W image of a $2.6 \times 1.4 \text{ kpc}^2$ region of M31's bulge.

2. PHAT data

We analyzed some of the first data available from the PHAT program (GO-12058) consisting of UV, optical, and IR imaging two 3×6 arrays of HST pointings with a 180° flip between each 3×3 subgrids. Each of these "bricks" corresponds to an area of $12' \times 6.5'$ ($2.6 \times 1.4 \text{ kpc}^2$; assuming a distance modulus of (m - M) = 24.47 from McConnachie *et al.* 2005). Brick 1 includes the center of M31 and Brick 9 is a disk field with galactocentric radius ~ 6.5 kpc. For full details of the PHAT observing strategy see Dalcanton *et al.* (in prep).

3. Matching known PNe with PHAT sources

Merrett *et al.* (2006, hereafter M06) provides the most extensive M31 PNe catalog to date, selected via low-dispersion spectra with the PNe Spectrograph. Their astrometry is good to ~ 0.2 arcsec. The catalog spatially covers the M31 disk up to ~ 30 kpc, though it is incomplete in the inner ~ 100 pc.

We cross-matched the PNe from the M06 catalog with the photometric catalogs for Bricks 1 and 9, (Fig. 1). The matched sources have mean positional offsets of Δ (RA) = -0.59'' and Δ (Dec) = -0.43'' between M06 and PHAT catalogs (Fig. 2). One typical identification is illustrated in Fig. 3, where the PN is evident as the brightest object in F475W; in these false-color F336W+F475W+F814W images, the PNe appear as green dots.

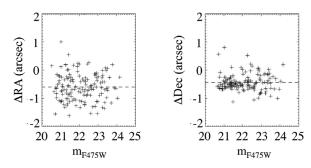


Figure 2. For 143 likely matches in Brick 1, RA/Dec offsets between PHAT and M06 positions ($\Delta = PHAT - M06$).

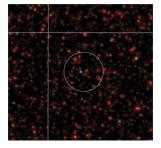


Figure 3. Example of a PNe observed in the outskirts of Brick 1. It appears as a greenish stellar-like object inside 1" radius circle around a M06 PN.

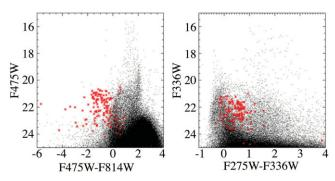


Figure 4. Distribution of Brick 1 PNe (asterisks) in two CMDs from PHAT, as compared to the underlying stellar population (dots). The PNe colors are all extremely blue in F475W–F814W.

4. Color magnitude diagrams

Fig. 4 shows the location of PNe in some example CMDs. The PNe are very blue in the optical. Within a box with limits F474W–F814W from -2 to 0, and F475W from 23.5 to 20.5, roughly 70% of the objects are PNe. The other 30% may be compact HII regions, symbiotic stars, AGN, or previously unidentified PNe.

5. Ongoing work and concluding remarks

We have models for the evolution of the emission lines in PNe, derived from rough approximations for their dynamical evolution (Marigo *et al.* 2001, 2004, plus Cloudy (Ferland *et al.* 1998) for deriving emission line fluxes). These models have been reprocessed using version 8.01 of Cloudy and then used for synthetic photometry in the PHAT filters.

Table 1 lists the dominant emission lines that enter the PHAT filters, and Fig. 5 shows the synthetic spectra derived from Cloudy, with a 10 Å resolution, for a solar-metallicity PNe model close to the peak of its $[OIII]\lambda 5007$ luminosity. We are now using these (and other) models to make predictions about the numbers and photometry of M31 PNe.

Besides the emission lines in Table 1, there are significant contributions from stellar, nebular H, and nebular He continuum in F275W and F336W, and significant Paschen continuum in F814W.

We are also comparing the radial surface density gradient of PNe with other sources in M31's bulge (Rosenfield *et al.*, submitted).

Our long term goal is to improve our understanding of the PNe progenitors and evolution. A crucial role in this project will be played by the spatially-resolved star formation history derived over 17 kpc of the M31 disk (Williams *et al.* in prep.), which is expected

ID	λ (Å)	\log Flux (cgs)	$\mathbf{Flux}/\mathbf{Flux}(\mathbf{H}eta)$	Filter
ΗI	4861	34.568	1.0000	F475W
ΗI	4340	34.240	0.4698	F475W
ΗI	4102	33.982	0.2597	F475W
ΗI	3970	33.769	0.1592	F475W
ΗI	12820	33.768	0.1585	F110W
He I	10830	33.835	0.1853	F110W
He I	10830	33.580	0.1029	F110W
He II	4686	34.658	1.2305	F475W
He II	3203	34.242	0.4725	F336W
He II	2733	33.955	0.2442	F275W
He II	2511	33.730	0.1453	F275W
He II	10120	34.109	0.3481	F110W
O III	5007	35.644	11.9229	F475W
O III	4959	35.165	3.9611	F475W
S III	9532	34.261	0.4941	F110W

Table 1. Partial list of relevant emission lines in PHAT filters

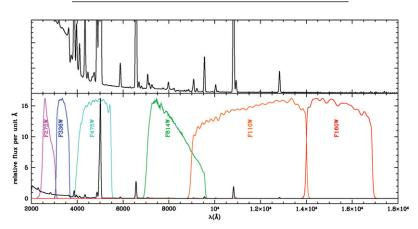


Figure 5. Model spectra of a PNe resulting from one of the Marigo *et al.* (2001) simple configurations combined with the photoionization code Cloudy, and compared to the transmission curves of PHAT filters. The top panel shows the same spectrum expanding the y-axis. The dominant feature in the spectrum is the [OIII] λ 5007 line falling in the F475W filter, but continuum emission does contribute at other wavelengths.

to correlate tightly with the specific numbers and observed properties of PNe. M31 represents a unique opportunity to study these correlations in a spiral galaxy similar to the MW.

To conclude: Although PHAT was not designed as a PNe survey, it provides (1) accurate astrometry and 6-filter photometry of known PNe, (2) a good number of (possible) new detections in the F475W filter, (3) new insights between the relation between PNe and UV-bright stars in M31 Bulge (Rosenfield *et al.* submitted, and in prep.), (4) excellent prospects for studying the PNe in relation with their progenitors across the whole disk.

References

Ciardullo, R., Jacoby, G. H., Ford, H. C., & Neill, J. D. 1989, ApJ, 339, 53
Ferland, G. J., Korista, K. T., Verner, D. A., et al. 1998, PASP, 110, 761
Marigo, P., Girardi, L., Groenewegen, M. A. T., & Weiss, A. 2001, A&A, 378, 958
Marigo, P., Girardi, L., Weiss, A., Groenewegen, M. A. T., & Chiosi, C. 2004, A&A, 423, 995
McConnachie, A. W., Irwin, M. J., Ferguson, A. M. N., et al. 2005, MNRAS, 356, 979
Merrett, H. R., Merrifield, M. R., Douglas, N. G., et al. 2006, MNRAS, 369, 120